



**HAL**  
open science

## High resolution pressure sensing using sub-pixel shifts on low resolution load-sensing tiles

Mihai Andries, François Charpillet, Olivier Simonin

► **To cite this version:**

Mihai Andries, François Charpillet, Olivier Simonin. High resolution pressure sensing using sub-pixel shifts on low resolution load-sensing tiles. 2015 IEEE International Conference on Robotics and Automation (ICRA 2015), May 2015, Seattle, United States. hal-01136255

**HAL Id: hal-01136255**

**<https://inria.hal.science/hal-01136255>**

Submitted on 27 Mar 2015

**HAL** is a multi-disciplinary open access archive for the deposit and dissemination of scientific research documents, whether they are published or not. The documents may come from teaching and research institutions in France or abroad, or from public or private research centers.

L'archive ouverte pluridisciplinaire **HAL**, est destinée au dépôt et à la diffusion de documents scientifiques de niveau recherche, publiés ou non, émanant des établissements d'enseignement et de recherche français ou étrangers, des laboratoires publics ou privés.

Copyright

# High resolution pressure sensing using sub-pixel shifts on low resolution load-sensing tiles

Mihai Andries<sup>1,2,3</sup>

François Charpillet<sup>1,2,3</sup>

Olivier Simonin<sup>4</sup>

**Abstract**—In ambient intelligence, pressure sensing can be used for detecting and recognizing objects based on their load profile. This paper presents a pressure scanning technique that improves weight-based object recognition, by adding information about the surface of the object in contact with the floor. The new high-resolution pressure scanning technique employs sub-pixel shifting to assemble a series of low-resolution scans into an aggregated high-resolution scan. The proposed scanning device is composed of 4 load-sensing tiles, on which the scanned object slides in regular movements. The result is a regular grid image of the object’s contact surface, containing the weight of each section of the grid, as well as the corresponding centers of mass. A formal proof-of-concept is provided, together with experimental results obtained both on a noiseless simulated platform, and on a noisy physical platform.

## I. INTRODUCTION

Ambient intelligence explores how sensing environments can interact with their inhabitants. We are interested in employing the sensors embedded in the environment for analyzing the activity of humans inhabiting it.

This work is a result of our exploration of load sensors’ capabilities. The goal is to recognize the actors and the activities performed on sensing surfaces by analyzing the forces perceived by the surfaces. Our previous work has centered on detecting, tracking and recognizing static and dynamic entities in the environment using load-sensing floors [1]. This was done in the context of the *Personally Assisted Living* Inria project, that aims to develop ambient and artificial intelligence for human assistance.

This paper presents a pressure scanning technique, which employs sub-pixel shifting to make a series of low-resolution scans, which are then assembled into a high-resolution scan. It exploits the information contained in the differences between the shifted scans, and aggregates this information to compute a composite pressure scan. The proposed pressure scanner architecture is composed of 4 load-sensing tiles. It calculates the weight transfer between the tiles when the analysed object slides over them. By using only the recorded mass and changements in the position of the center of mass, the scanner is able to reconstruct the contact surface of the object that slid on it. It also calculates the distribution of weight inside the surface of contact.

M. Andries is supported by an Inria CORDIS grant within the Personally Assisted Living Inria Project Lab. This work has been funded by Region Lorraine and Inria.

<sup>1</sup>Inria, Villers-lès-Nancy, 54600, France

<sup>2</sup>Université de Lorraine, LORIA, UMR 7503, Vandoeuvre-lès-Nancy, 54506, France

<sup>3</sup>CNRS, LORIA, UMR 7503, Vandoeuvre-lès-Nancy, 54506, France

<sup>4</sup>CITI-Inria Laboratory, INSA Lyon, 69621 Villeurbanne, France

The rest of the paper is organized into 4 sections. Section II presents the previous work on sub-pixel shifting and other related techniques. Section III describes the scanning equipment required for obtaining pressure scans, and introduces the algorithm that aggregates the scanning data. In section IV, we describe the results we obtained through simulation on a noiseless platform, as well as results obtained experimentally, on a physical platform subject to noise. Section V draws a conclusion and presents the perspectives of this work for home automation and its applications for industrial settings.

## II. RELATED WORK

High-resolution pressure scanning is usually performed using high-resolution pressure sensing devices (such as [4] and [8]). These often have a non-negligible price tag, due to the high number of embedded sensors. This paper demonstrates that high-resolution pressure scanning is also feasible using a low-resolution sensor and techniques such as sub-pixel shifting, something which has not yet been attempted, to our knowledge.

Similarities can be identified between the pressure-sensing and imaging domains. The pressure perceived by a load-sensing surface is analogous to the amount of light perceived by an image-recording sensor. Both in imaging and pressure sensing, the sensor can be shifted by less than a pixel width to register a slightly different part of the incoming light or pressure. Two such sub-pixel shifted images, aligned along one of the two axes of the scan, can be assembled into a higher-resolution image, using the information gathered by the sub-pixel shift.

Such imaging techniques that construct a high-resolution image from several low-resolution images containing sub-pixel shifts have been proposed by Peleg et al. [5], Keren et al. [3], Tekalp et al. [9] and Tom et al. [10].

The pressure sensor can also be composed of only one load-sensing tile, within a grid of other tiles that simply serve as physical support for the scanned object. Depending on how the object is placed on the sensing tile, the scanner will perceive new pressure data with every object placement that differs from the previous ones. Coupled with a system for identifying the displacement of an object’s bounding box (e.g., a cartesian coordinate robot), it can be considered as the canonical scanner of such type, as it consists of a single detection element. A scanner equivalent in functionality while lacking the cartesian robot will be described in section III-A.

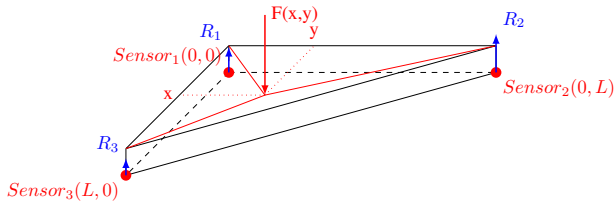


Fig. 1: Load distribution on an isostatic tile

The 1-sensing-tile scanner can be viewed as a single detection element scanner, for which the tiles that simply support the scanned object have the role of an aperture, that decides what portion of the object will be detected. This idea has been exploited in imaging, where a grid-like aperture was used to selectively allow light to pass through the aperture grid.

For instance, Huang et al. [2] used an LCD screen as an aperture in their implementation of the single detection element camera. The pixels of the LCD screen could turn transparent or non-transparent (black) to the incoming light, allowing different parts of the image to be perceived. The resolution of the obtained composite image was dependent on the resolution of the LCD screen used as aperture.

Both technologies (single detection element with a high-resolution aperture, sub-pixel shifts of the aperture) can potentially be combined to compute images with even higher resolution.

### III. METHODOLOGY

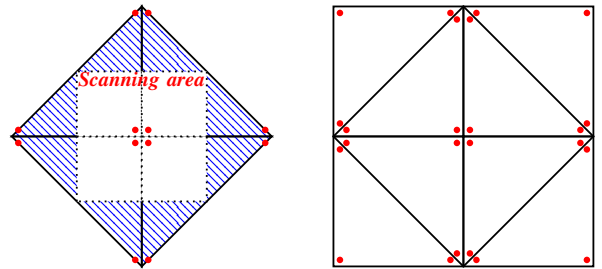
#### A. Scanning equipment

The instrument we use for scanning is constructed of 4 isostatic load-sensing tiles (see Fig. 1). The benefit of isostatic load-sensing tiles is the capability to calculate unambiguously the distribution of load on the sensors supporting the tile. The tiles are assembled so as to have vertical and horizontal frontiers between them, that will measure the flow of mass between the tiles (see Fig. 2). This type of scanner architecture can scan the contact surface of objects with size up to one fourth of the total scanning surface.

For clarity reasons, in the rest of the paper we will consider that the scanner is composed of only 4 square scanning parts, corresponding to the effective scanning area seen in Fig. 2a.

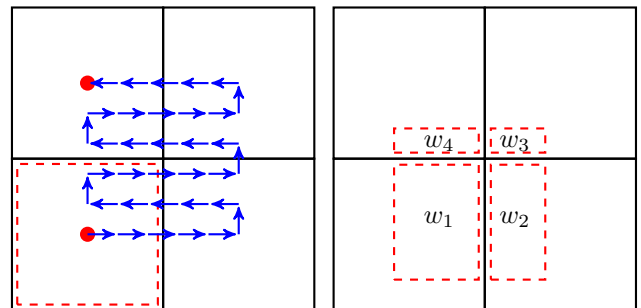
The object to be scanned is slid in a boustrophedon manner, with alternative horizontal and vertical translation movements over the plates (see Fig. 3a), allowing the entire object surface to be scanned. After each translation movement, the tiles measure the weight and calculate the coordinates of the center of pressure for the object portion standing on them (see Fig. 3b). Thus, at each step, the 4 tiles generate a low-resolution 4-sliced image of the load on the contact surface. These images are then assembled into a single grid-like high-resolution image of the contact surface (see Fig. 4b).

The displacement brought by each translation can be measured by tracking the center of pressure of the object on



(a) Scanner with 4 isostatic tiles, which employs only half of the tiles' scanning surface. (b) Scanner with 8 isostatic tiles, which employs all the scanning surface of the tiles.

Fig. 2: Examples of scanners with isostatic load-sensing tiles. The load sensors are represented as red dots.



(a) Sliding the object in a boustrophedon manner over the scanning surface. The object's bounding box is highlighted in red. (b) Each scan generates a 4-sliced image of the weight-distribution inside the object's bounding box.

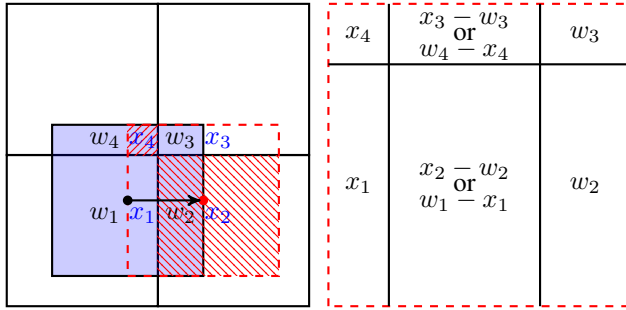
Fig. 3: Object scanning methodology

the scanning surface. The coordinates of the object's center of pressure will correspond to the coordinates of the center of mass of a system of particles composed by the sensors of the scanner, where each particle's mass is proportional to the weight perceived by the corresponding sensor. The distance travelled by the object's center of pressure corresponds to the distance travelled by its bounding box.

The translation movements can be performed by a cartesian coordinate robot (like the one presented in [7]), if the goal is to achieve high precision. For less precise scanning, the object can even be translated by hand, and scanned once the translation movement is completed and no exterior forces act on the object.

The problem can be schematically reduced to determining the weight of each pixel in the load-image representing the contact surface of the analysed object (see Fig. 4). Any given two load images can be assembled into a higher resolution image if both are subdivided by a common  $x$  or  $y$  line. This line is used for aligning the two images, creating the additional high-resolution image subdivisions.

The scanning resolution can be modified by changing the object shifting step: bigger steps lead to less gathered information, and therefore to lower-resolution final scans,

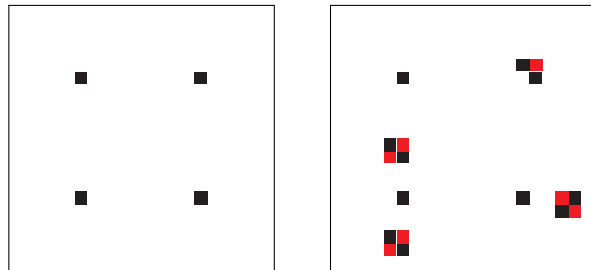


(a) Overlapping of two low-resolution load images. (b) Aggregate of two overlapping low-resolution load images.

Fig. 4: Construction of a high-resolution image from low-resolution images.

and vice versa. The maximum spatial resolution depends on three factors: the precision of the object translation, the sensitivity of the pressure sensor, and the sensor noise. The noise level of the sensor must be inferior to the recorded pressure value in each pixel. This means that a noisy sensor will be able to make high-resolution scans only for heavy objects.

The object translation movements must not be accompanied by rotations, as they skew the scanned load images, preventing them from aggregating into a sharp, non-ambiguous load-distribution image. Considering the gradual calculation of the pressure scan image, the errors are cumulative, propagating themselves through the scan. Fig. 5 presents an example of skewing due to object rotation.



(a) The expected scan figure, without skewing. (b) Example of scan image skewing, obtained while scanning with a 10% chance of rotating the figure by 5 degrees.

Fig. 5: Example of skewing a scan image by rotation of the scanned object. Positive pressure values are represented in grayscale, while negative pressure values are shown in shades of red. Skewing generates negative pressure values, that counterbalance the additional pressure points detected.

The scanning speed depends on the speed of object manipulation, and on the measuring frequency of the sensor. Due to the presence of sensor noise, several measurement must be made from which the most probable pressure value is calculated.

For example, a system able to translate the scanned object at a speed of 1 translation per second, and taking 1 second to measure the weight of the object on the scanner, scanning an object of size  $1 \text{ m}^2$ , with a resolution of  $1 \text{ cm}^2$ , would require 10 000 measurements, which would take 5.5 hours to record. Scanning the same object at a resolution of  $10 \text{ cm}^2$  would require 100 measurements, and take only 3 minutes 20 seconds of time.

### B. Scanning algorithm

Each scan of the object generates 4 pieces of information, provided by the 4 tiles of the scanner (see Fig. 3b), that contain: the coordinates of the scanned object portion, the weight of this object portion, and the center of pressure of this portion.

The scanned pieces of the object are stored in a list of type `objectPiece`. Each `objectPiece` contains 6 fields: the  $x$  and  $y$  axes that bound it (`xLeft`, `xRight`, `yTop`, `yBottom`), its weight, and the coordinates of the center of pressure. These object pieces are then assembled into a high-resolution image using the pressure-image registration algorithm described hereafter.

Each time a new piece of the object bounding box is scanned, the algorithm checks if this piece contains or is contained by another known piece. If the new piece contains another known piece, the surface and weight of the latter is subtracted from the new piece, thus reshaping the new object piece that has to be added to the scan. If the new piece is contained by another known piece, the latter is split in 2: the new piece, and the piece obtained by subtracting the new piece from the one already known.

Performing this type of scanning while moving the object in a regular manner generates a pressure grid. Fig. 6 offers an intuition on the way the algorithm executes itself.

The pressure-image registration algorithm is presented in pseudocode in Algorithm 1. Its worst case complexity is quadratic in the number of object pieces already scanned. This can be reduced to linear complexity by comparing only pieces that share 3 common bounds. For clarity reasons, this optimization was omitted in the paper.

The boustrophedon algorithm simply moves the object as shown in Fig. 3a, and generates the corresponding scan after each translation. This procedure, that allows all the sections of the object to be scanned, is detailed in Algorithm 2. The boustrophedon algorithm has a complexity of  $\mathcal{O}(1)$  in the desired scan resolution.

## IV. EXPERIMENTAL RESULTS

Experiments have been done both using a simulator of load-sensing tiles that we developed for our work on sensing floors for ambient intelligence, and using a real-world implementation of the scanner. These experiments are detailed in the following sections.

### A. Scanning simulation

As presented in section III-A, the scanner was simulated using 4 load-sensing tiles. The object to be scanned was represented using a set of pressure points, which correspond

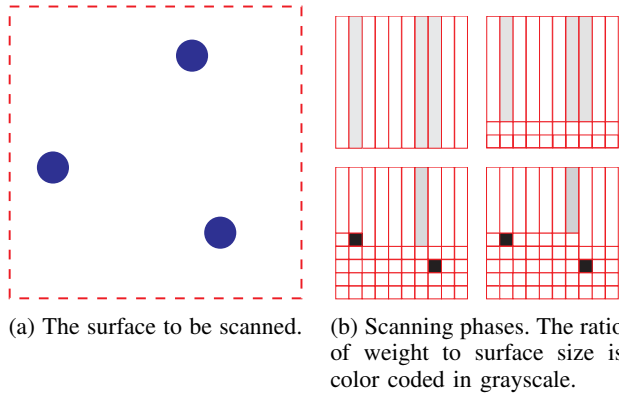


Fig. 6: Sample scan execution on a simulator. As the scanning progresses, the pressure image gets richer in detail.

to the surface of the object in contact with the scanner (see Fig. 7a).

By translating the object following a boustrophedon trajectory, we obtain a pressure scan of the object’s surface in contact with the scanner, as shown in Fig. 7. The scan result for an object with different pressure intensities inside its contact surface is presented in Fig. 8. These pressure differences were represented as grayscale intensities in the final result.

Given that the sensing tiles can not only weigh the portion of the object they support, but also calculate the center of pressure for that portion, the pressure scans can be augmented using information about the centers of pressure in each cell of the pressure-grid scan.

### B. Physical experiment

The physical experiment was implemented on a scanner composed of square sensing tiles. These tiles are 60 cm x 60 cm in size, made of 3.8 cm thick wood, and are mounted on a floating floor structure that supports them. Each tile is equipped with 4 load sensors (one in each corner, as shown in Fig. 9b). This equipment is described in more detail in [6] and [1]. Although these tiles are non-isostatic, this has not hindered the experimental results.

The scanned object was a chair, weighing 5 kg, and with the chair legs forming a trapezoid shape (see Fig. 9a). Given the high level of noise on our platform ( $\pm 2.5$  kg), the chair was loaded with additional 40 kg of weight disks, to generate a pressure scan that would be easily discernable from noise.

First, the tiles were calibrated, after which the average zero-pressure value was recorded for each load-sensing tile, when no objects were placed on the scanner. This served as reference for the ulterior measurements.

The scanned object was then placed on the scanner and weighed by each load-sensing tile. The pressure values for each of the 4 tiles were calculated by averaging the pressure values over 50 measurements (which takes 1 second at 50 Hz with the current prototype). The position of the object was measured by hand using the millimeter paper. It could not be done automatically by calculating the position of the center of pressure, because the load sensors were subject to noise,

---

### Algorithm 1 Pressure-image registration algorithm

---

```

1: procedure ADDPIECE (newObjPiece)
2:   if newObjPiece.hasZeroSurface then
3:     return;
4:   else if listOfObjPieces.isEmpty() then
5:     listOfObjPieces.add(newObjPiece);
6:   else
7:     for each objPiece in listOfObjPieces do
8:       if newObjPiece.contains(objPiece) then
9:         croppedObjPiece =
10:          newObjPiece.subtract(objPiece);
11:         addPiece(croppedObjPiece);
12:         return;
13:       else if objPiece.contains(newObjPiece) then
14:         croppedObjPiece =
15:          objPiece.subtract(newObjPiece);
16:         listOfObjPieces.remove(objPiece);
17:         listOfObjPieces.add(newObjPiece);
18:         listOfObjPieces.add(croppedObjPiece);
19:         return;
20:       end if
21:     end for
22:   end if
23: end procedure

```

---



---

### Algorithm 2 Boustrophedon pressure scan

---

```

1: procedure BOUSTROPHEDON
2:   repeat
3:     scanObject();
4:     if !canMoveObjectLeft() then
5:       while canMoveObjectRight() do
6:         moveObjectRight();
7:         scanObject();
8:         addPiece(topLeftPiece);
9:         addPiece(topRightPiece);
10:        addPiece(bottomLeftPiece);
11:        addPiece(bottomRightPiece);
12:      end while
13:     else
14:       while canMoveObjectLeft() do
15:         moveObjectLeft();
16:         scanObject();
17:         addPiece(topLeftPiece);
18:         addPiece(topRightPiece);
19:         addPiece(bottomLeftPiece);
20:         addPiece(bottomRightPiece);
21:       end while
22:     end if
23:     if canMoveObjectDown() then
24:       moveObjectDown();
25:     end if
26:   until !canMoveObjectDown()
27: end procedure

```

---

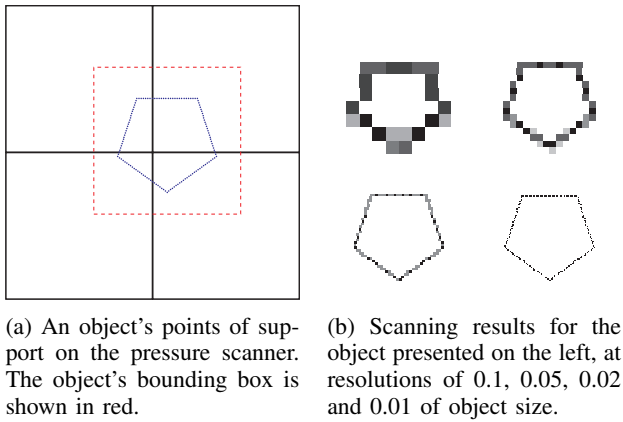


Fig. 7: Scan simulation for a pentagonal object surface and the resulting scan.

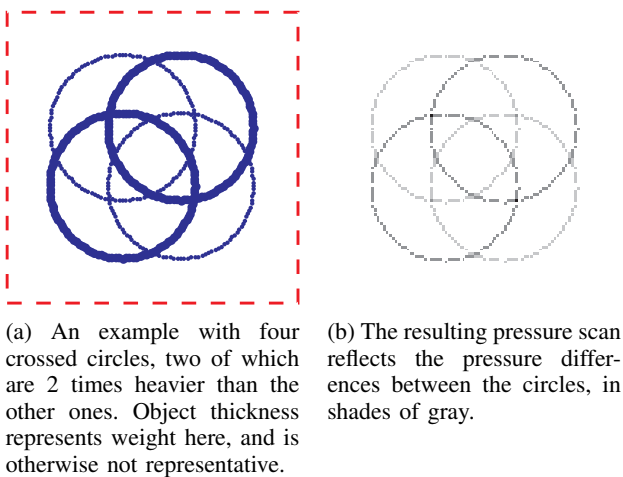


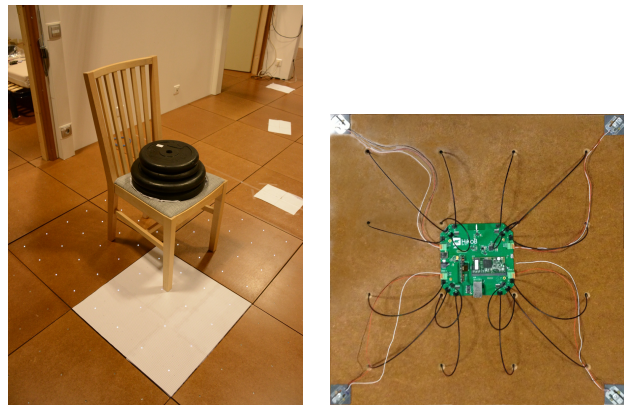
Fig. 8: Scan simulation for a non-trivial object shape.

which would have prevented the alignment of measurements into a grid. The translations were carefully done by hand, which also constituted a possible source of error.

Due to the manual translation required for each measurement, the experiment, which consisted of 100 measurements, lasted for 2 hours. The duration of the experiment, combined with the load placed on the tiles (45 kg) introduced hysteresis-related errors towards the end of the experiment. However, according to the sensor specification, this error is bounded to 0.03% of the full scale measurement, and is thus negligible.

The results of the scan are presented in Fig. 9c and 9d. The noise present in the scan is related to the sensor noise, and was removed using a rough threshold filter, with a threshold set at 2x the noise of an individual sensor. Noise filtering done using a statistical model of the sensor noise should yield even finer results.

Unfortunately, the sensor noise on our current platform ( $\pm 2.5$  kg) did not allow us to scan objects with a more complex surface (containing more than 10 pixels), as this would have required them to be too heavy to manipulate.



(a) A chair being scanned on a scanner made of 4 load-sensing tiles. One tile was covered in millimeter paper, to be used as a location reference. Translations were performed by hand.

(b) The underneath of the load-sensing tiles used, showing the load sensors located in the corners.



(c) The pressure scan obtained without noise filtering. Most of the noise is caused by sensor noise. The highest pressure is encoded as black.

(d) The pressure scan obtained with noise filtering. The perceived pressure is rendered as an equivalent weight value at 1G acceleration.

Fig. 9: Physical implementation of the pressure scanner.

### C. Open questions

There is no proof that the boustrophedon trajectory is optimal in terms of highest gain of information in the lowest possible number of translations of the object. Finding the optimal (quickest) trajectory for scanning an object with the described sensor in order to find the geometry and the pressure in each point of its contact surface remains an open question.

It would also be interesting to scan objects that don't move in a regular fashion, but which are augmented by an orientation sensor. These objects can be scanned at the moments when their orientation matches with the one required by the scanner.

Fine-grained noise filtering using a statistical model of the noise is also of great interest for these platforms. It would allow to greatly improve the accuracy of measurements, enabling pressure scanning for more lightweight objects.

## V. CONCLUSION AND PERSPECTIVES

This paper presents a new type of high-resolution pressure scanning technique, which employs sub-pixel shifting on a low-resolution load sensor to generate and assemble a high-resolution pressure scan. The proposed scanner architecture is composed of 4 load-sensing tiles, on which the scanned object is translated vertically and horizontally in a boustrophedon manner using sliding moves. A formal proof-of-concept was provided, together with a set of experimental results obtained on a noiseless simulator and on a physical implementation of the scanner.

This system could be used for measuring the weight distribution on surfaces. For instance, on transportation lanes, it can check for abnormalities in weight distribution between the front and rear driving axles of vehicles. The same applies for railroad tracks, where it can measure the weight distribution of the rolling stock. In an industrial setting, this technique could be used for measuring the density in each slice of a block of metal or other material.

It can also be used as a floor sensor in sensing environments, recognizing mobile objects by their surface in contact with the ground. In the context of sensing environments equipped with floors consisting of this type of load-sensing tiles, this scanning system could provide a way for obtaining footprints, thus offering input data for human recognition algorithms.

Pressure surface scanning provides a new way of interpreting load data, which is distinct from the common *ground reaction force* profile interpretation. It improves weight-based object recognition, adding information about the floor projection of the object's shape.

## REFERENCES

- [1] Mihai Andries, François Charpillet, and Olivier Simonin. Object recognition on load-sensing floors modeled as a multiple knapsack problem. *IEEE Sensors Journal*, under review, 2014.
- [2] Gang Huang, Hong Jiang, Kim Matthews, and Paul Wilford. Lensless imaging by compressive sensing. *arXiv preprint arXiv:1305.7181*, 2013.
- [3] D. Keren, S. Peleg, and R. Brada. Image sequence enhancement using sub-pixel displacements. In *Computer Vision and Pattern Recognition, 1988. Proceedings CVPR '88., Computer Society Conference on*, pages 742–746, Jun 1988.
- [4] H. Morishita, R. Fukui, and T. Sato. High resolution pressure sensor distributed floor for future human-robot symbiosis environments. In *Intelligent Robots and Systems, 2002. IEEE/RSJ International Conference on*, volume 2, pages 1246 – 1251 vol.2, 2002.
- [5] Shmuel Peleg, Danny Keren, and Limor Schweitzer. Improving image resolution using subpixel motion. *Pattern Recognition Letters*, 5(3):223 – 226, 1987.
- [6] Nicolas Pepin, Olivier Simonin, and François Charpillet. Intelligent Tiles: Putting Situated Multi-Agents Models in Real World. In ACM AAAI, editor, *International Conference on Agents and Artificial Intelligence - ICAART'09*, Porto, Portugal, 2009.
- [7] D. Slater and F. Mitchell. High precision cartesian robot for a planar scanner, December 5 2002. US Patent App. 09/873,907.
- [8] Prashant Srinivasan, David Birchfield, Gang Qian, and Assegid Kidane. Design of a pressure sensitive floor for multimodal sensing. In *Proceedings of the Ninth International Conference on Information Visualisation, IV '05*, pages 41–46, Washington, DC, USA, July 2005. IEEE Computer Society.
- [9] AM. Tekalp, M.K. Ozkan, and M.I Sezan. High-resolution image reconstruction from lower-resolution image sequences and space-varying image restoration. In *Acoustics, Speech, and Signal Processing, 1992. ICASSP-92., 1992 IEEE International Conference on*, volume 3, pages 169–172 vol.3, Mar 1992.
- [10] B.C. Tom and AK. Katsaggelos. Reconstruction of a high-resolution image by simultaneous registration, restoration, and interpolation of low-resolution images. In *Image Processing, 1995. Proceedings., International Conference on*, volume 2, pages 539–542 vol.2, Oct 1995.